QUAZI Z-SOURCE INVERTER INCORPORATED WITH HYBRID RENEWABLE ENERGY SOURCES FOR MICROGRID APPLICATIONS

R. SATHISHKUMAR[1], V.MALATHI[2], P.DEEPAMANGAI[3]

[1,2,3] Anna University, Regional Campus Madurai, INDIA

[1]rskeee@autmdu.ac.in, [2]vmeee@autmdu.ac.in, [3]deepamangaipalanivel@gmail.com.

ABSTRACT: *With the incursion of renewable energy into the power generation system, the demand for Energy storage system (ESS) becomes significant. Hence, parallel operation of Battery Energy Storage Systems (BESS) is an important application in microgrids. The quasi-Z-source inverter (qZSI) with BESS can poise the random wavering of power from renewable sources injected to the load or grid. The qZSI is a single stage converter with two controllable DC ports. The batteries connected in the two DC ports of qZSI are charged by hybrid renewable energy resources such as solar and wind energy. Due to the volatile nature of renewable sources, the batteries may be supplied with unequal voltage and current ratings. These BESS with different voltage and power rating supplies the load, hence a proper control strategy is required to accomplish the current sharing between these batteries. The proposed control strategy is investigated in both islanded mode and grid connected mode. Also the maximum power point tracking (MPPT) methods are used to harvest maximum power from solar and wind energy systems. This will ensure maximum conversion efficiency.*

Keywords: *qZSI, hybrid renewable energy resources, Wind, PV, MPPT, Proportional resonant (PR) controller*.

1. Introduction

To operate the distribution networks in a controllable manner, microgrids are incorporated in power generation. These microgrids play an important role in electrical power generation system due to increasing use of distributed energy resources (DESs). This microgrid is incorporated with energy sources and all types of loads. The energy sources may be renewable sources and storage equipments which are connected to the sources through power electronic converter stages. The microgrid can function either independently or connected to main grid. With the increasing penetration of renewable energy resources, the ESS is becoming an integral part of the future electrical systems bringing many technical and financial benefits to these systems. Usually, to integrate ESSs into conventional electricity grids, one needs to design special topologies and/or controllers for almost each particular case. The ESSs have the competence to work either in charging mode or in discharging mode.

There are various problems associated with microgrid development such as efficiency, stability and power quality issues. To alleviate this issues ESS has been proposed as a solution [1-3]. The arrangements of battery system for high level of power and energy capacity in microgrids has many problems such as in case of series arrangement of batteries, if one battery fails it may interrupt other batteries, thereby leading to parallel operation [4-5]. The power conversion stage is an important stage in microgrid to regulate the DC voltage to a desirable value, the qZSI intriguing the gain of the shoot-through duty cycle [5]. This feature of qZSI has provided the advantage of using BESS in parallel arrangement and also incorporating the features of renewable sources [6-7]. The parameters of qZSI are important criteria for proper operation of batteries, hence the battery parameters are chosen in such a way to reduce the battery current ripples in microgrid applications [8-13]. In microgrid, there may be dispatchable and non-dispatchable renewable resources may be present causing unbalanced load, and hence PR controller is used to track the reference with zero steady state error under dynamic behavior of system [14]. Photovoltaic (PV) generation has received special attention nowadays as one of the major energy sources of the future because of its flexible configuration, less fuel cost and eco-friendly nature [15]. However, the output power induced in the PV modules depends on variation in temperature, radiation, internal factors, and partial shading, etc. [16]. Therefore, only for one specific operating point, the maximum power output is obtained from the solar panel just for one specific operating point.

The efficiency of the PV generation depends on maximum power extraction of PV system. The PV array has a distinctive operating point that can supply maximum power to the load [17]. In order to operate the PV array at its maximum power point (MPP), the PV system must contain a MPPT controller. Many MPPT algorithms have been proposed in recent years. The conventional algorithms such as perturb & observe (P&O), Incremental conductance (INC) work satisfactorily only under uniform irradiation conditions in which PV curve has a unique MPP [18].

The output power of the PV will vary by the surrounding conditions such as irradiation and temperature. Recently artificial intelligence methods which include Fuzzy logic controller (FLC) Artificial Neural Network (ANN) and Adaptive neuro-fuzzy inference system controller (ANFIS) have been applied to track MPP [19]. The ANN based MPPT to alleviate the problem of oscillation around MPP and there is no need for the prior knowledge of the PV parameters [20]. The dataset for the ANN is obtained from experimental measurements.

In the proposed system discussed in paper this paper, the batteries connected in the two DC ports of qZSI are charged by renewable energy resources such as solar and wind energy. The PR control strategy is used to reduce the steady state error to zero. Also ANN MPPT and Hill climbing MPPT are used to harvest maximum power from solar and wind energy systems respectively.

2. RENEWABLE ENERGY SOURCES

Hybrid renewable energy system usually consists of two or more renewable sources such as wind and PV. Nowadays HRES are used to overcome the unforeseen nature of renewable energy sources especially wind system. Both wind and solar can be combined to use as HRES because both have the capability to supply power in remote areas and also they are eco-friendly in nature. To provide an unintermittent power supply to the load significant amount of battery bank is needed which is connected in the dc ports of qZSI.

2.1 Photovoltaic System

A photovoltaic (pv) system converts solar energy into electricity. The PV cells absorb photons of light and release electron charges are the canonic of PV technology. The desired output power from PV is obtained by connecting PV modules in series or parallel. The equivalent circuit of PV cell is shown in Figure1.

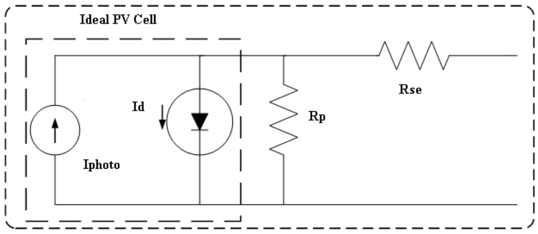

Figure 1: Equivalent model of the PV panel

The current equation is given in Equation (1).

$$I = I_{pv} - I_0 \left[exp \frac{qv}{akT} - 1 \right] \quad (1)$$

Where,

I_{pv} = PV current,
T = Temperature,
a = Diode ideality constant,
I_0 = leakage current of the diode,
q = charge of an electron (1.6021×10^{-19} C)
k = Boltzmann constant (1.38×10^{-23} J/K).

The Equation (1) represents the basic equation of ideal photovoltaic cell. To get the desired output voltage from PV panel, numbers of PV cells are connected in series, since a single PV cell can produce less than one volt.

The short-circuit current (I_{SC}) depends on insolation according to Equation (2).

$$I_{SC}(Irr) = \left(\frac{Irr}{Irr_0} \right) I_{SC}(Irr_0) \quad (2)$$

where,

I_{rr} = irradiation and

I_{rr0} = standard irradiance at standard operating condition (1000 W/m^2).

The BP SX 150 PV module is used for simulation. The PV module is modeled and simulated in MATLAB as per the datasheet of BP SX 150 PV module and the values are given in Table 1. To get the desired voltage of 200 V, 5modules are connected in series. The VI curve is shown in Figure 2.

Table 1: BP SX 150S PV panel parameters

PARAMETERS	VALUE
P_{max}	150W
V_{mpp}	34.5V
I_{mpp}	4.35A
V_{oc}	43.5V
I_{sc}	4.75A

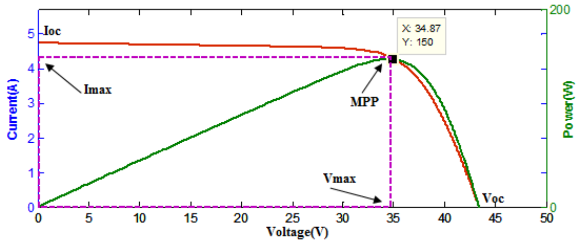

Figure 2: VI curves of BPSX 150s PV module with MPP

The Simulation diagram of PV system is shown in figure3.

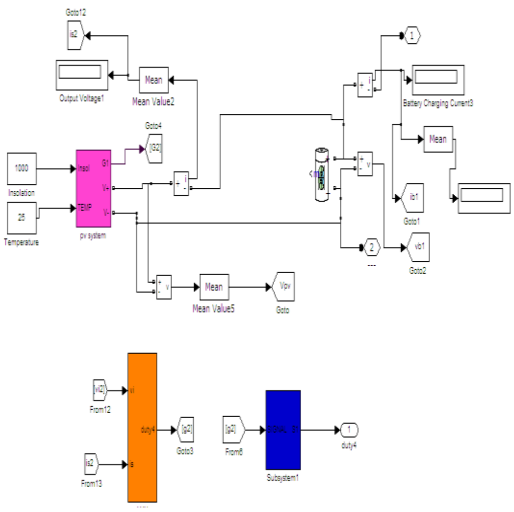

Figure 3: Simulink diagram of PV system

The energy extracted from solar is eco friendly in nature and it also varies with atmospheric condition as well. The maximum conversion efficiency is obtained only when maximum power is extracted from PV panels. The tracking of MPP under different atmospheric conditions such as variation in irradiance and temperature is a complex task. Hence, several MPPT algorithms have been developed to obtain MPP. In order to investigate our proposed work, the PV system is modeled under non-shaded condition and ANN MPPT is used to track MPP. The PV insolation is changed from 1000 W/m^2 to 800 W/m^2 in 0.1 sec. and the corresponding MPP voltage is shown in Figure 4.

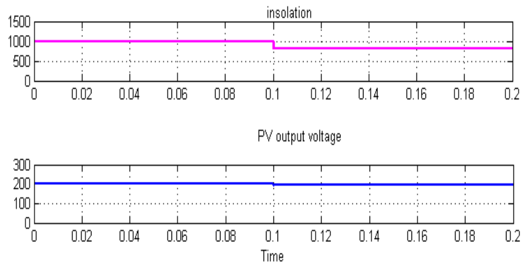

Figure 4: Insolation and PV output voltage

2.2 Modeling of Wind Turbines

The wind turbine is modeled as in [21]. The kinetic energy of the air particles can be expressed in Equation (3).

$$E = \frac{1}{2}\rho\pi r^2 V^3 t \qquad (3)$$

where,

E, is the kinetic energy of the moving air,
m is the total mass of the air particles,
V is wind speed.
ρ is the air density
A is the swept area of the wind turbine rotor.
r is the radius of the wind turbine rotor.

The actual wind power (P_w) at any instant of time ‘t’ can be mentioned in Equation (4).

$$P_w = \frac{E}{t} = \frac{1}{2}\rho\pi r^2 V^3 \qquad (4)$$

The Betz relationship is given by,

$$C_p = \frac{P_T}{P_W} \qquad (5)$$

Where, P_T is the mechanical power captured by the wind turbine,

C_p is the power coefficient of the wind turbine

$$C_p = c_1(c_2 \frac{1}{\alpha} - c_3\beta - c_4\beta^x - c_5)e^{-c_6 \frac{1}{\alpha}} \quad (6)$$

where,

$$\frac{1}{\alpha} = \frac{1}{\lambda + 0.08\beta} - \frac{0.035}{1+\beta^3} \quad (7)$$

and,

$$\lambda = \omega_m r / V \quad (8)$$

Where,

α is the blade angle

β is the tip speed ratio of the wind turbine, ω_m is the angular speed of the wind turbine generator. The simulation of wind energy system is shown in Figure 5.

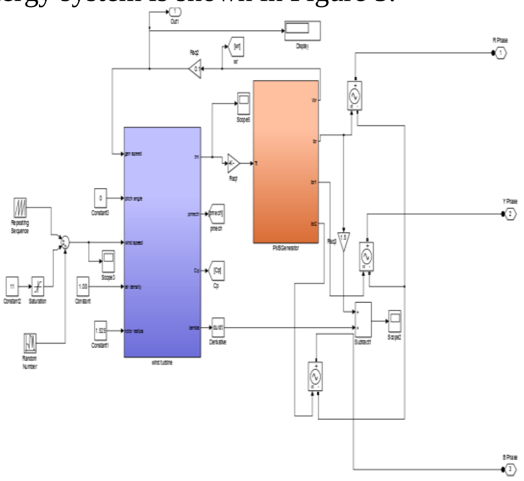

Figure 5: Simulation diagram of wind energy system

The values of the coefficients (C_1-C_6) depend on the type of the wind turbine. To maximize the power, a control system for the adjustment of the blade angle for different wind conditions is desirable for the wind turbine. Hence the power captured by the wind turbine can be rewritten as in Equation (9).

$$P_T = \frac{1}{2}\rho\pi r^2 C_p(\lambda,\beta)V^3 \quad (9)$$

To directly drive the wind power generation systems and to transform the mechanical power into electrical power, a permanent magnet synchronous generator (PMSG) is ideal and well suited. The mathematical model of PMSG is derived as in [21].

The input electrical power for PMSG is given in Equation (10),

$$P_{dq} = \frac{3}{2}(v_{ds}i_{ds} + v_{qs}i_{qs}) \quad (10)$$

The mechanical power is expressed as Equation (11)

$$P_{em} = \frac{3}{2}(e_d i_{ds} + e_q i_{qs}) \quad (11)$$

where,

$$e_d = -\omega_e L_q i_{qs} = -\omega_e \lambda_q$$

$$e_q = -\omega_e L_q i_{qs} = -\omega_e \lambda_q$$

$$T_e = \frac{3}{2}\left(\frac{p}{2}\right)(\lambda_r i_{qs} + (L_d - L_q)i_{qs}i_{ds}) \quad (12)$$

Where p is number of poles of the machine.

3. PROPOSED SYSTEM

The block diagram of proposed system is shown in Figure 6.

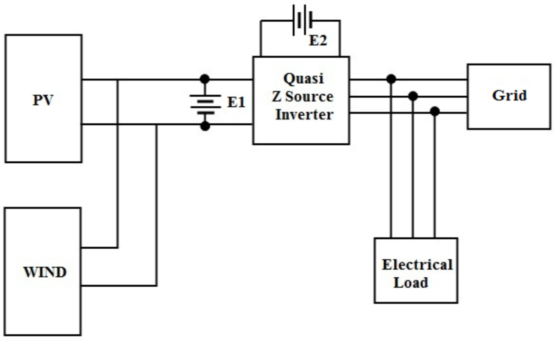

Figure 6: Block diagram of proposed system

The QZSI is a single stage converter and boost the input voltage of PV by its unique shoot-through state characteristic. To connect the AC loads or main grid, certain AC voltage level is needed. Hence the QZSI is advantageous in economical point of view to interface unforeseeable renewable energy sources with AC loads as it is a single stage circuit. The circuit diagram of qZSI is shown in Figure 7. The zero states (000 or 111) of conventional modulation schemes are replaced by shoot through and non shoot-through states. The shoot-through duty ratio as $d_O = T_0 / Ts$, where T_0 is the shoot through interval among switching cycle T_s.

At Steady state,

$$V_{dc} = V_{C1} + V_{C2} = \frac{1}{1-2d_0} V_{in} \qquad (13)$$

Where

$$V_{C1} = \frac{1-d_0}{1-2d_0} V_{in}$$

$$V_{C2} = \frac{d_0}{1-2d_0} V_{in}$$

V_{C1}, V_{C2} are the capacitor voltages in QZSI

V_{dc} is the DC link voltage.

The conditions for boost control methods are,

$MI \le 1 - d_0$ for normal boost

$MI \le \frac{2}{\sqrt{3}}(1-d_0)$ for boosting maximum constant voltage

$MI \le \frac{2\pi}{3\sqrt{3}}(1-d_0)$ for maximum boost

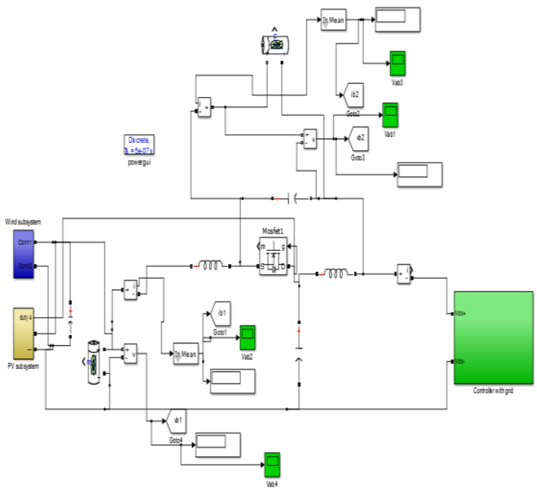

Figure 7: Simulation diagram of qZSI

It is perceptible, that the inverter legs are applied with both shoot through duty cycle and MI. Hence it is difficult to design a controller, since these two parameters depends on each other. The large value of d_0 but a small value of *MI* increases voltage stress across devices and is not economical. Hence PR control strategy is proposed to overcome the above shortcoming and also to fulfill the current sharing of two batteries operated under different voltage and power ratings. The simulation of quasi Z source inverter is shown in Figure 7.

4. CONTROLLERS

The controllers used for PV, wind and qZSI are ANN MPPT, Fuzzy MPPT and PR controller respectively.

4.1 ANN MPPT controller

ANN is the model of the human brain that attempts to mimic its learning process. It is an intelligent adaptive system that changes its configuration based on input and output information. ANN model consists of neurons in three layers viz input, hidden and output layers. The input layer is activated by external information. The output layer delivers the results to an external device. The hidden layers lie between the input and output layers.

The ANN is trained in such a way that to track the MPP of a particular PV module at any insolation and temperature, the ANN should give a reference MPP voltage that corresponds to the maximum power. The training data sets are obtained from experimental results with the temperature varying from 20 to 50° C and solar insolation varying from 50 to 1000 W/m^2. There are two input nodes voltage and current and one output node, the reference MPP voltage and 10 hidden layers. The activation function is sigmoid. The simulation diagram of ANN MPPT system is shown in Figure 8.

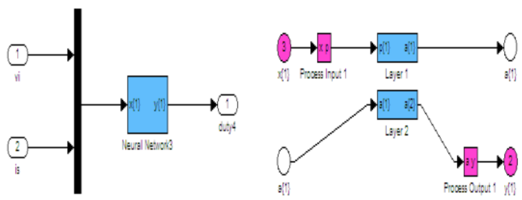

Figure 8: Simulation diagram of ANN MPPT systems

In figure 9, shows that 2000 set of patterns are used for training and testing, which consists of PV insolation (G), temperature (T) and MPP reference voltage (V_{ref}).In this data set, 70% of samples is used for training and remaining is used for testing and validation. The performance of this trained ANN is analyzed in terms of mean square error (MSE). The Structure of ANN network is shown in figure 10, this modeled ANN is satisfactorily working i.e it gives the nearest reference MPP voltage to achieve the MPP for given insolation and temperature, when MSE is nearer to zero. The tan sigmoid function is used as the activation function.

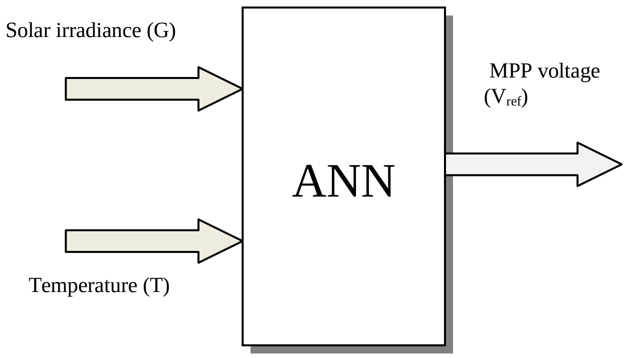

Figure 9: Block diagram of ANN MPPT

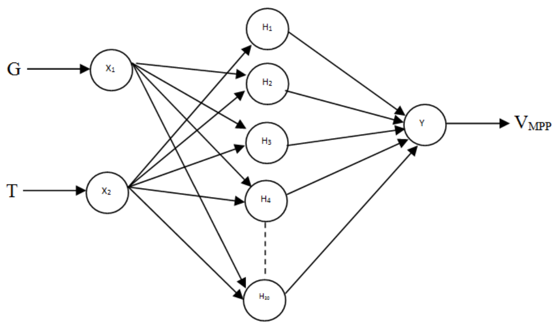

Figure 10: Structure of ANN network

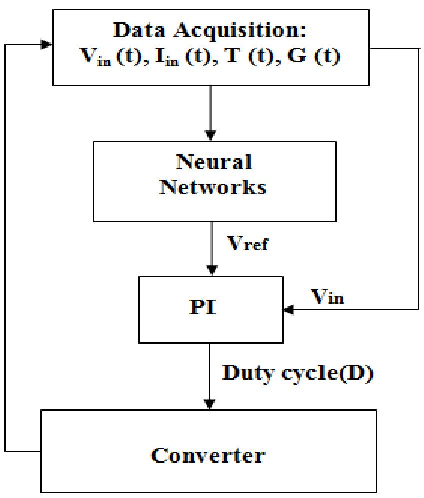

Figure 11: ANN MPPT systems

Figure 11 shows of ANN MPPT systems. The performance is measured by calculating the mean- square error as shown in Equation. (14).

$$MSE = \frac{1}{td}\sum_{k=1}^{td}\left\| y^{(k)} - v_{ref}{}^{(k)} \right\|^2 \qquad (14)$$

Where, td= number of training data entries; y = ANN output vector; v_{ref} = output

The system reaches this v_{ref} using PI controller.

The PI control law is of the form following Equation (15).

$$u(t) = K_p.e(t) + K_i \int_0^t e(t)dt \qquad (15)$$

Where,

K_p-proportional gain,

K_i-integral gain

The PI controller output the duty cycle based on the error.

4.2 Fuzzy MPPT for Wind

Fuzzy logic uses human experience and the human experience is put into the control scheme and plays an important part in decision making in the elimination of error. Fuzzy logic is a procedure to deal with approximate data to arrive at an agreeable result. It is applicable wherever the data available is approximate but within practically useful limits, the system being nonlinear and that importantly the system could be settled within the agreeable limits of accuracies of results.

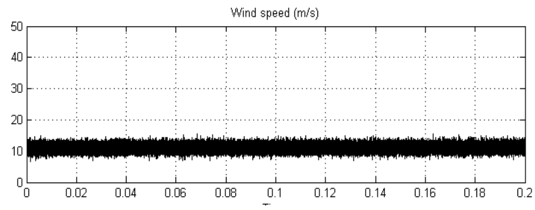

Figure 12: Variable wind speed

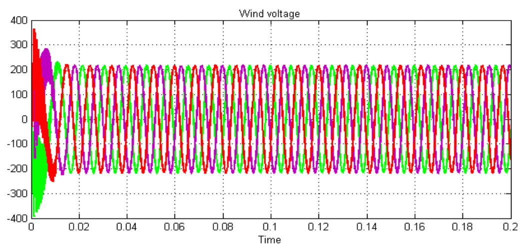

Figure 13: Output Voltage from wind

In the first phase of the fuzzy logic a fuzzification process is carried out and using the fuzzified data at hand a rule base is applied to arrive at the region of vicinity of the solution. Then using this data the process moves on to the next phase where a crisp result is found by way of the process called defuzzification. The rule matrix is shown in Table 2.

Table 2: Fuzzy rule matrix

Error / ***Error rate***	**NB**	**NS**	**ZE**	**PS**	**PB**
NB	NB	NB	NB	NS	ZE
NS	NB	NB	NS	ZE	PS
ZE	NB	NS	ZE	PS	PB
PS	NS	ZE	PS	PB	PB
PB	ZE	PS	PB	PB	PB

The wind speed is randomly varied between 8 m/s^2 to 12 m/s^2 as shown in Figure 12 and the corresponding output voltage is shown in Figure 13.

4.3 PR Controller

The AC-side controller operates in stationary $(\alpha\beta)$ reference frame, the proportional PR controller can be used to track the reference values with zero steady-state error endowed with a suitable dynamic behavior. The PR controller transfer function is given in Equation (16),

$$PR = K_P + \frac{K_R s}{s^2 + \zeta s + \omega^2} \qquad (16)$$

where,

ω is microgrid frequency

ζ is the cut off frequency

K_P and K_R are PR controller parameters obtained by stability analysis as depicted in Table 3.

Table 3: Controller parameters

PARAMETERS	**VALUE**
K_R	400
K_P	1
ω	8 π rad/sec
ξ	0.8

In islanded microgrid, the switch is in position “0” and the reference current for the AC current controller is provided by the AC voltage controller. In this mode, the battery currents are predicted by the load power demand. The shoot-through duty cycle is the key parameter in the proposed current sharing algorithm. In the grid-connected mode, the BESS must operate in the current control mode. In this mode, the selector switch is in position “1” and the output current of battery systems is regulated to their references provided by the BESS management system. The simulation diagram of PR controller is shown in Figure 14.

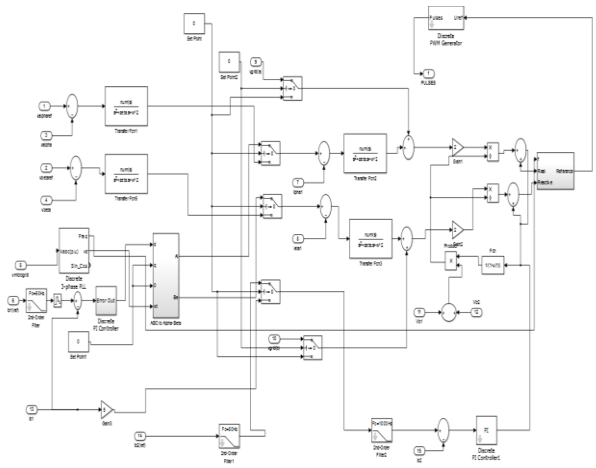

Figure 14: Simulation diagram of PR controller

The current of battery1 is regulated by adjusting the inverter AC current, while the current of battery2 is regulated using the shoot-through duty cycle. The current controller of battery2 is designed considering a certain bandwidth and stability margins using the current controller model. Considering the current controller of battery2 is designed with kpb2= $-3.3 \times 10^{-3}$and kib2= −0.67 providing a bandwidth of 531 Hz with the phase margin and gain margin of 31.4∘and 70.1 dB, respectively, as shown in Figure 15. The unbalanced load may cause oscillatory power and also cause ripples in battery current as double times its microgrid frequency. The current controller of battery2 has a bandwidth higher than 100 Hz enabling it to track 100 Hz oscillatory reference current with a zero steady-state error. Hence the batteries may share current appropriately the load currents.

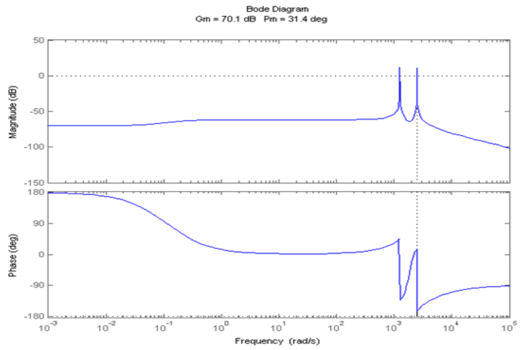

Figure 15: Bode plot of battery current controller

5. RESULTS AND DISCUSSION

MATLAB/Simulink is used to validate the proposed system. The qZSI system parameters are tabulated in Table 4.

Table 4: System parameters

PARAMETERS	VALUE
Inductance (L1, L2)	400 μH
Capacitance C	600 μF
Cp1, Cp2	400 μF
Switching frequency	20 kHz
Battery rating (equal)	200 V, 6.5 Ah
Battery rating (unequal)	B1: 200 V,6.5 Ah, B2=120 V, 12.5 Ah

The Wind and PV power are varied with the wind speed, reference voltage, and the DC link voltage is maintained at 400V which is the voltage boosted by qZSI impedance circuit which is shown in figure 18. In both the cases the irradiation and wind speed are varied and a step change in load is applied at 0.1 sec real power changed from 2 kW to 4 kW and reactive power changed from 4 kVAr to 8 kVAr. The grid voltage and current is shown figure 16 and also qZSI inverter output voltage and current is shown if figure 17.

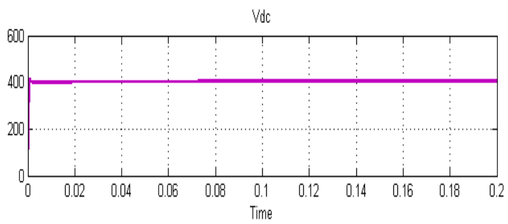

Figure 16: DC link voltage

In both the cases of battery rating, the sudden increase in real and reactive power is met out by grid as well as by renewable sources as shown in Figure 19.

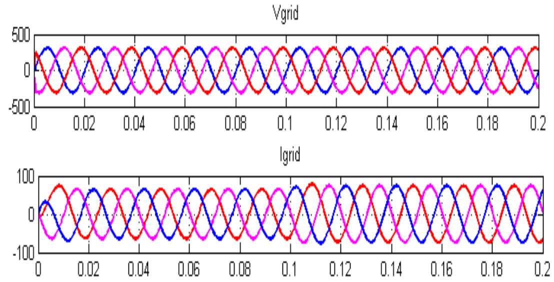

Figure 17: Grid voltage and current

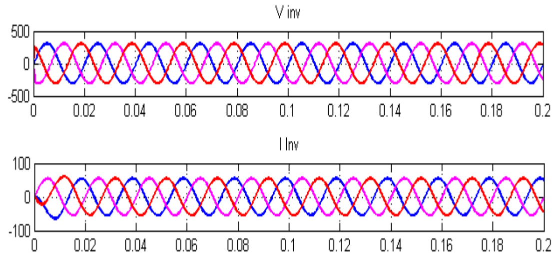

Figure 18: qZSI inverter output voltage and current

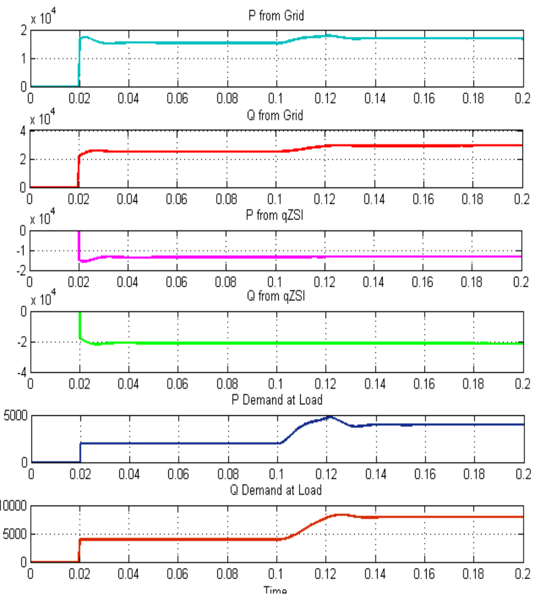

Figure 19: Power flow

Case I. Equal voltage and current ratings

Figure 20 shows the results when two battery systems have the same voltage rating of 200 V. The two battery systems are energized by PV and wind. The insolation and wind speed are set such that the same power is extracted from wind and PV. Initially, the total load of the microgrid is supposed to be 2 kW and 4 kVar. At t = 0.1sec, the total load power is increased to 4 kW and 8kVar. From the Figure, it is clear that the battery system shares equal current ratings irrespective of the load power changes and the load voltage also regulated by AC voltage controller.

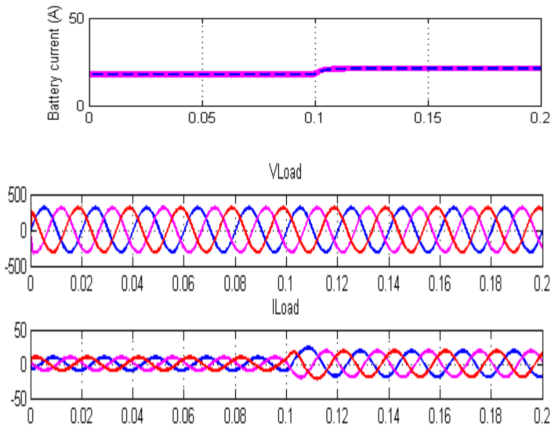

Figure 20: Battery, Load voltage and current for equal voltage and current rating of batteries

Case II. Different voltage and current ratings

Figure 21 shows the results when two battery systems have the different voltage rating of 200 V and 120 V and also have different current rating is shown in Figure 21.

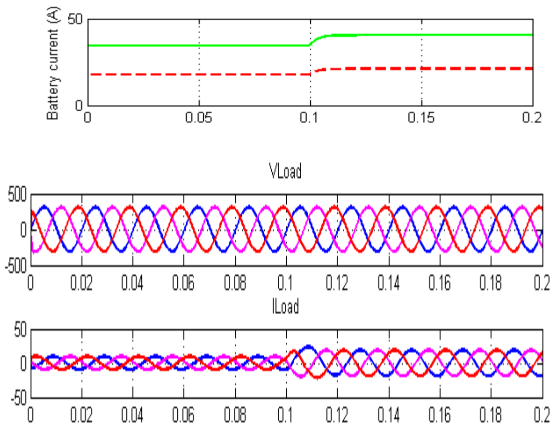

Figure 21 : Battery, Load voltage and current for unequal voltage and current rating of batteries

The battery systems are energized by PV and wind. The battery 1 may have 1.5 times the current of battery 2. The load changes scenario is same as in previous case and the batteries also share the load current in proportion to their current ratings. The qZSI is operated in such a way that load voltage is regulated irrespective of load changes.

6. CONCLUSION

The modeling and control strategy for qZSI for parallel operation of BESS in microgrids was presented. The proposed control strategy is investigated and also the MPPT schemes are incorporated to harvest maximum power from solar and wind energy systems in order ensure maximum conversion efficiency. The proposed method provides the use of hybrid renewable energy sources and its maximum power extraction for energy storage devices. The proposed method is validated in MATLAB/Simulink for a typical microgrid implying two battery systems exemplified by different current and voltage ratings.

REFERENCES

[1] Caldognetto, T., Tenti, P., Costabeber, A., Mattavelli, P.: *Improving microgrid performance by cooperative control of distributed energy sources*. In: IEEE Trans. Ind. Appl. 50 (6) 2014, 3921–3930.

[2] Adhikari, S., Li, F.: *Coordinated V-f and P-Q control of solar photovoltaic generators with MPPT and battery storage in microgrids*. In: IEEE Trans. Smart Grid. 5 (3), 2014, 1270–1281.

[3] Wasiak, R., Pawelek, R., Mienski.: *Energy storage application in low-voltage microgrids for energy management and power quality improvement*. In: IET Trans. Gener. Transm. Distrib. 8 (3), 2014, 463–472.

[4] Moo, C.S., Ng, K.S., Hsieh, Y.C.: *Parallel operation of battery power modules*. In: IEEE Trans. Energy Convers. 23 (2), 2008, 701–707.

[5] Anderson, J., Peng, F.Z.: *Four quasi-Z-source inverters*. In: Proc. of IEEE PESC, Jun 2008, pp. 2743–2749.

[6] Ge, B., Abu-Rub, H., Peng, F.Z., Lei, Q., de Almeida, A.T., Ferreira, F.J.T.E., Sun, D., Liu, Y.: *An energy-stored quasi-Z-source inverter for application to photovoltaic power system*. In: IEEE Trans. Ind. Electron. 60 (10), 2013, 4468–4481.

[7] Liu, Y., Ge, B., Abu-Rub, H., Peng, F.Z.: *Control system design of battery-assisted quasi-Z-Source inverter for grid-tie photovoltaic power generation*. In: IEEE Trans.Sustainable Energy 4 (4), 2013, 994–1001.

[8] Liu, J., Jiang, S., Cao, D., Peng, F.Z.: A *digital current control of quasi-Z-Sourceinverter with battery*. In: IEEE

Trans. Ind. Inf. 9 (2) (2013) 928–937.

[9] Loh, P.C., Vilathgamuwa, D.M., Gajanayake, C.J., Lim, Y.R., Teo, C.W.: *Transient modeling and analysis of pulse-width modulated Z-source inverter*. In: IEEE Trans. Power Electron. 22 (2), 2007 498–507.

[10] Liu, J., Hu, J., Xu, L.: *Dynamic modeling and analysis of Z-source converter—derivation of AC small signal model and design oriented analysis*. In: IEEE Trans. Power Electron. 22 (5), (2007, 1786–1796.

[11] Pogaku, N., Prodanovic, M., Green, T.C.: *Modeling, analysis and testing of autonomous operation of an inverter-based microgrid*. In: IEEE Trans. Power Electron. 22 (2), 2007, 613–625.

[12] Li, Y., Jiang, S., Rivera, J.G.C., Peng, F.Z.: *Modeling and control of quasi-Z-source inverter for distributed generation applications*. In: IEEE Trans. Ind. Electron. 60(4) (2013) 1532–1541.

[13] Hamzeh, M., Karimi, H., Mokhtari, H.: *A new control strategy for a multi-bus MV microgrid under unbalanced conditions*. In: IEEE Trans. Power Syst. 27 (4), 2012, 2225–2232.

[14] Bidram, A., Davoudi.: *Hierarchical structure of microgrids control system*. IEEE Trans. Smart Grid. 3 (4), 2012, 1963–1976.

[15] Jasem Khajesalehi, Mohsen Hamzeh, Keyhan Sheshyekani, Ebrahim Afjei.: *Modeling and control of quasi Z-source inverters for parallel operationof battery energy storage systems: Application to microgrids*.In: Electric Power Systems Research. 125, 2015, 164–173.

[16] Bader, N, Alajmi, Khaled H, Ahmed, Stephen J, Finney & Barry W Williams: *A Maximum Power Point Tracking Technique for Partially Shaded Photovoltaic Systems in Microgrids*. In : IEEE transactions on Industrial Electronics, vol.60 (2013), pp.1596-1606.

[17] Villalva, MG., Gazoli, JR & Filho, ER.: *Comprehensive approach to modelling and simulation of photovoltaic arrays*. In: IEEE Transactions on Power Electronics, vol. 24, no. 5, 2009, pp. 1198-1208.

[18] Hohm DP & Ropp ME: *Comparative study of maximum power point tracking algorithms using an experimental, programmable, maximum power point tracking test bed*. In: Proceedings of Photovoltaic Specialist Conference, 2000, pp.1699-1702.

[19] Chokri Ben Salah & Mohamed Ouali: *Comparison of fuzzy logic and neural network in maximum power point tracker for PV systems*. In: Electric Power Systems Research, 2011, vol. 81, pp.43-50.

[20] Whei-Min Lin, Chih-Ming Hong & Chiung Hsing Chen. *Neural network based MPPT control of a stand-alone hybrid power generation system.* In IEEE Transactions on Power Electronics, vol.26, 2011, pp.3571-3581.

[21] Busca, C., Stan, A. I., Stanciu, T., Stroe, D. I.: *Control of permanent magnet synchronous generator for large wind turbines.* In: Proceedings of IEEE-ISIE2010, 2010, pp. 3871–3876.